Featured in Physics

Bending to Kinetic Energy Transfer in Adhesive Peel Front Microinstability

V. De Zotti,[1] K. Rapina,[1] P.-P. Cortet,[2] L. Vanel,[3] and S. Santucci[1,4,*]
[1]Université de Lyon, ENSL, UCBL, CNRS, Laboratoire de Physique, F-69364 Lyon, France
[2]Laboratoire FAST, CNRS, Université Paris-Sud, Université Paris-Saclay, F-91405 Orsay, France
[3]Université de Lyon, Université Claude Bernard Lyon 1, CNRS, Institut Lumière Matière, F-69622 Villeurbanne, France
[4]Lavrentyev Institute of Hydrodynamics, Novosibirsk, Russia

(Received 17 July 2018; revised manuscript received 9 November 2018; published 15 February 2019)

We report an extensive experimental study of a detachment front dynamics instability, appearing at microscopic scales during the peeling of adhesive tapes. The amplitude of this instability scales with its period as $A_{\mathrm{mss}} \propto T_{\mathrm{mss}}^{1/3}$, with a prefactor evolving slightly with the peel angle θ, and increasing systematically with the bending modulus B of the tape backing. Establishing a local energy budget of the detachment process during one period of this microinstability, our theoretical model shows that the elastic bending energy stored in the portion of tape to be peeled is converted into kinetic energy, providing a quantitative description of the experimental scaling law.

DOI: 10.1103/PhysRevLett.122.068005

The periodic velocity oscillations of the detachment front during the peeling of adhesive tapes constitute an archetypal example of a dynamical rupture instability. This stick-slip motion leads to a screechy sound that everyone has experienced, when peeling off packing tape. However, despite a large number of studies [1–12], this instability is not fully understood and still causes industrial problems, with deafening noise levels, and damages to both adhesives and peel systems.

The effective fracture energy of adhesive-substrate joints can decrease over certain ranges of peel front velocity [2–5]. In such an unstable condition, for which less energy is required for the crack front to propagate faster, a transition from a quasistatic rupture mode to a dynamic one occurs, as for frictional interfaces [13–15]. During the rapid slip phases, the dynamical mode of failure is likely to give rise to small scale spatiotemporal front instabilities [16]. Indeed, ultrafast imaging could unveil that the peel front locally advances by steps in the main peel direction as a result of the propagation of a dynamic fracture kink in the transverse direction at spatiotemporal scales much smaller than the macroscopic stick slip [17–19]: the kink occurs periodically at ultrasonic frequencies with an amplitude of a few hundred microns, not only during the slip phase of the macroinstability, but also for imposed peel velocities in a finite range beyond the macro-stick-slip domain where the peeling is regular at macroscopic scales [19].

Interestingly, this microinstability of the peel front characterized by the sideways propagation of fracture kinks share similarities with other physical processes, as, for instance, the local contact line dynamics on textured surfaces [20], or the dislocations motion in the yielding of crystalline materials [21]. While it was shown that those transverse cracks are accompanied by cycles of load and release of the elastic bending energy stored in the tape backing in the vicinity of the peel front [19], the physical origin of the microinstability and its interaction with the macroscopic one remains an open issue.

In this Letter, we provide a detailed experimental study of this microinstability, varying systematically the peeled length L, the peel angle θ, the lineic mass μ, and bending modulus B of the ribbon, over a wide range of driving peel velocities V. Thanks to a large data statistics, we show that the microinstability amplitude scales with its period as $A_{\mathrm{mss}} \propto T_{\mathrm{mss}}^{1/3}$, with a prefactor that increases with the bending modulus of the tape backing. We demonstrate that the bending elastic energy of the ribbon released during each microslip is converted into kinetic energy, allowing a quantitative prediction of this scaling law.

We peel a 3M Scotch® 600 adhesive tape from a transparent flat substrate by winding its extremity at a constant velocity V with a brushless motor. Changing the relative position of the substrate and peeling motor, we can easily vary the peel angle θ and ribbon length L. The peeling of this tape (a polyolefin blend backing $b = 19$ mm wide, $e = 34$ μm thick, tensile modulus $E = 1.41$ GPa, density $\mu = 8.10^{-4}$ kg/m) coated with a 15 μm synthetic acrylic adhesive layer has been widely studied [4–6, 17–19,22–25]. In contrast with those studies, for each experiment, using a scalpel, we carefully extract two layers of the adhesive tape from its original roller. We attach them on a transparent plate and then, perform the peeling at the interface between those two layers. The release side of the adhesive tape backing constitutes the top part of the substrate of our peel experiments. Thanks to the homogeneous properties of the commercial roller adhesive layer, this protocol improves the reproducibility of our

 © 2019 American Physical Society

experiments, by avoiding a pre-peeling, which may damage the adhesive.

A Photron SA5 fast camera with a macrolens images a small portion of the peel front through the transparent substrate with a resolution of 9.8 μm/pixel, at a rate of 175 000 or 300 000 fps, for 640×56 and 832×24 px^2 images, respectively. Analyzing the gray levels of each image, we extract the detachment front longitudinal position x at a given transverse position z. During an acquisition, this front typically advances a few mm, so that L and θ can be considered constant (varying less than 5%). A sketch of the setup can be found in the Supplemental Material [26] together with typical recorded videos.

In the driving velocity range $[V_a, V_d]$ [27], for which the peel force decreases, the detachment front displays the classical stick-slip instability, with regular velocity oscillations at the millisecond timescale, and millimetric slips related to cycles of loading and release of the stretching energy stored in the whole peeled tape. The oscillating front velocity is thus different from the driving velocity V imposed at the extremity of the peeled tape, which is the control parameter of the experiment. When the mean front velocity (measured at the ms timescale) becomes larger than $v_a \simeq 1$ m/s [28], the peel front advances by the propagation of fracture kinks, across the tape width, in the transverse direction z, at very high velocities, from 650 up to 900 m/s [19]. Those dynamic transverse cracks occur during the slip phase of the macroinstability, but also permanently, as shown in Fig. 1, for driving velocities above V_d, the disappearance threshold of the macroinstability. This microinstability finally disappears as well, when the mean peel front velocity is above $v_d \simeq 20$ m/s [19]. Figure 1 gives a typical example of the local front

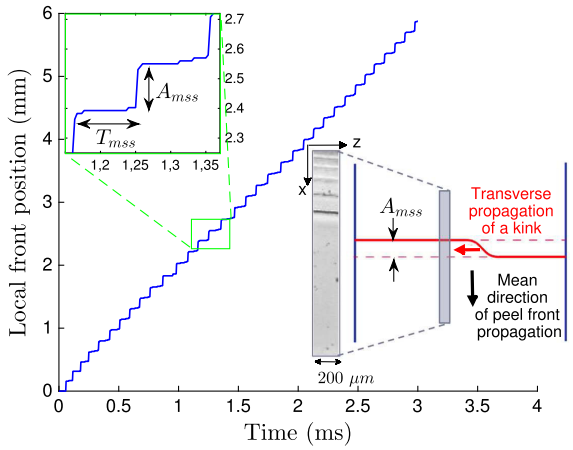

FIG. 1. Micro-stick-slip dynamics of the local longitudinal position of the peel front during an experiment at $V = 1.8$ m/s, $L = 50$ cm, and $\theta = 90°$, with periods of rests T_{mss} preceding slips of size A_{mss}, as a result of the transverse propagation across the tape of a kinked fracture of amplitude A_{mss}. We also display a typical image recorded by the fast camera (the gray zone in the inset gives its reduced field of view).

position time series for an experiment at $V = 1.8$ m/s, $L = 50$ cm, $\theta = 90°$. While the average front velocity measured at the ms timescale is equal to the driving velocity V (regular peeling without microscopic stick-slip), at shorter timescales we observe a staircase dynamics with sudden jumps of amplitude $A_{\mathrm{mss}} \simeq 170$ μm separated by periods of rest of $T_{\mathrm{mss}} \simeq 100$ μs.

From the peel front temporal evolution measured for each experiment, we could detect several thousands of micro-stick-slip events. For each of them, we extract the period of rest T_{mss} preceding a microslip of amplitude A_{mss}. In Fig. 2 (top), we display A_{mss} as a function of T_{mss}, averaged in logarithmic bins. We gather here data of numerous experiments: for a fixed peel angle $\theta = 90°$ and several peeled ribbon length L (inset), and changing this angle θ while keeping L fixed to 50 cm (main panel). We clearly observe that A_{mss} increases with T_{mss}, following a power-law scaling with an exponent close to $1/3$, independent of the peeled length L (inset). On the other hand, both the range and prefactor of the scaling law evolve slightly with the peel angle (inset, bottom panel), but seemingly not the power-law exponent.

In order to evaluate the role of the elastic bending energy, stored locally in the vicinity of the peel front, we have studied the impact of the ribbon bending modulus B.

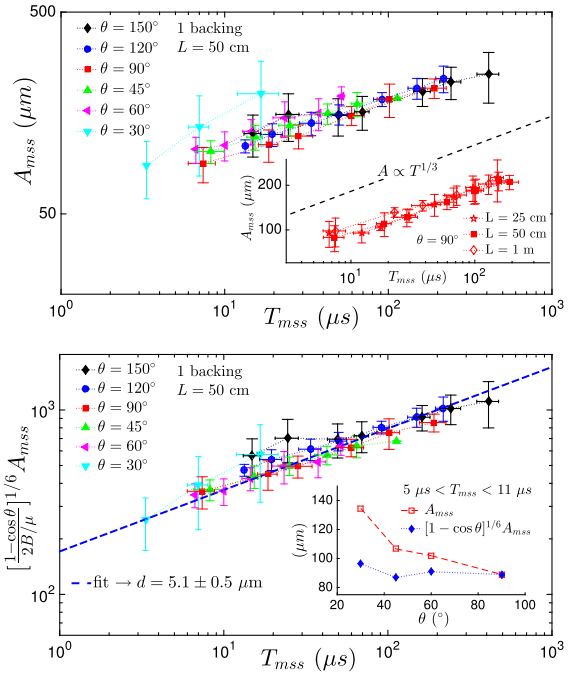

FIG. 2. Mean amplitude of the microscopic stick-slip A_{mss} as a function of the mean duration T_{mss} for a wide range of experimental conditions at different peel velocities: different peel angle θ at $L = 50$ cm and for $\theta = 90°$ and three peeled lengths L (inset). The bottom panel shows the same data but with A_{mss} rescaled by $\{2B/[\mu(1-\cos\theta)]\}^{1/6}$ following Eq. (2). The inset shows that the microslips' amplitude associated to periods $T_{\mathrm{mss}} \in [5, 11]$ μs evolve as $(1-\cos\theta)^{-1/6}$.

Superimposing up to 4 layers of the 3M Scotch® 600 rigid backing (cleansed of its adhesive coating) with a rigid glue (using $e_L = 26 \pm 10$ μm layers of Loctite® 406), we could increase the bending modulus of our adhesive tape by 2 orders of magnitude. Indeed, considering that the n-layer backing of thickness $h_n = ne + (n-1)e_L$ has the same tensile modulus E than the 3M Scotch® 600 ribbon, its bending modulus can be estimated as $B = Eh_n^3 b/12$. As a result, we find a systematic increase in the microslips size A_{mss} with B, as shown in Fig. 3 (inset), preserving nevertheless the $T_{\mathrm{mss}}^{1/3}$ scaling.

We discuss now the evolution of the adhesive tape close to the peel front, in order to obtain a local energy balance of the detachment process during a microscopic stick-slip cycle (per unit width of the peel front). During the microstick phase, the adhesive layer is stretched, while the ribbon is bent locally at the vicinity of the static detachment front. We assume that a microslip of size A_{mss} occurs suddenly, when the glue is stretched up to a critical length d. During this fast interfacial crack propagation, both the elastic bending energy of the ribbon E_{B-r} and the stretching energy of the glue E_{S-g} stored during the microstick phase are released. Therefore, we can write the local energy balance during a microscopic stick-slip

$$E_{B-r} + E_{S-g} = \Gamma A_{\mathrm{mss}} + E_k, \tag{1}$$

where Γ is the effective fracture energy of the adhesive-substrate joint, and E_k corresponds to the excess of elastic energy released, converted into kinetic energy that the tape locally acquires. Such energy balance is similar to the one proposed by Mott [29], generalizing Griffith's criterion [30] to describe dynamic rupture processes.

The effective fracture energy Γ has been theoretically related to the energy needed to deform the adhesive layer up to a critical strain at which it debonds [31–33]. Recent experiments with polyacrylate adhesives have shown that this energy is indeed proportional to the integral of the nonlinear rate-dependent stress-strain curve of the confined glue [34]. The critical elongation of the glue at debonding d is thus a crucial parameter in the determination of the peeling energy Γ (the value of d and its dependencies with material, geometrical, and dynamical parameters is still an open issue [34–36]). In this context, we can consider that the energy accumulated in the deformation of the glue E_{S-g} is completely dissipated when it debonds and a microslip of size A_{mss} occurs, i.e., $\Gamma A_{\mathrm{mss}} = E_{S-g}$. As a consequence, the local energy balance (1) leads to the transfer of the ribbon bending energy E_{B-r} into an increase of kinetic energy E_k that the tape locally gains during a micro-slip, $E_{B-r} = E_k$.

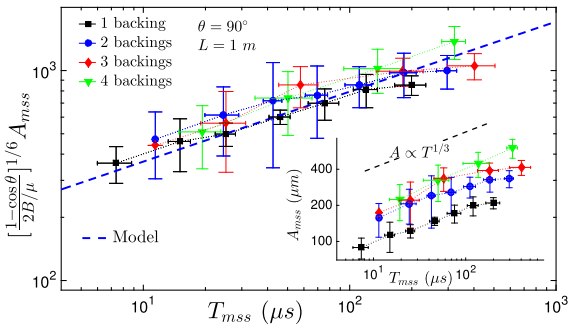

FIG. 3. Mean amplitude of the microscopic stick-slip A_{mss} as a function of the mean duration T_{mss} for peel experiments at $L = 1$ m and $\theta = 90°$, with tape of different ribbon thicknesses measured in numbers of superimposed glued backings.

Assuming that the tape is bent over a length scale equal to the microslip size A_{mss}, just before its triggering at the critical elongation of the glue d, with a radius of curvature $R_0 \simeq A_{\mathrm{mss}}^2/2d$, the order of magnitude of the bending energy released during a micro-slip writes $E_{B-r} \simeq \frac{1}{2} B A_{\mathrm{mss}}/R_0^2 \simeq 2Bd^2/A_{\mathrm{mss}}^3$. In our model, the micro-slip duration is fixed by the timescale for the release of this local bending energy E_{B-r}, controlled *a priori* by the bending waves period $\tau = [\lambda^2/(2\pi)]\sqrt{(\mu/B)}$ [37] of wavelength $\lambda = A_{\mathrm{mss}}$. Considering a single tape layer with $\lambda \sim$ 150–200 μm gives a timescale $\tau \sim 0.3$–0.6 μs, much smaller than the micro-stick-slip period T_{mss}, in agreement with our measurements. Therefore, in this approach, the fracture kink transverse propagation proceeds at the group velocity $v_g = 2\lambda/\tau$ of bending waves of wavelength $\lambda = A_{\mathrm{mss}}$. The estimated velocities ($650 \to 900$ m/s) are also in excellent agreement with the experimental reported values [19].

On the other hand, the increase of kinetic energy that the tape locally gains during a microslip is $E_k = \frac{1}{2}\mu A_{\mathrm{mss}}(A_{\mathrm{mss}}/T_{\mathrm{mss}})^2 2(1-\cos\theta)$. In this formula, the factor $2(1-\cos\theta)$ results from the motion of the tape just beyond the curved region, which is a combination of a translation in the direction θ at $V_{\mathrm{mss}} = A_{\mathrm{mss}}/T_{\mathrm{mss}}$ and a translation at the same velocity in the direction of the peel front motion [25]. Finally, the transfer of bending to kinetic energy $E_{B-r} = E_k$ allows us to link the amplitude and period of the microscopic stick-slip:

$$A_{\mathrm{mss}} = \left(\frac{2B/\mu}{1-\cos\theta}\right)^{1/6} d^{1/3} T_{\mathrm{mss}}^{1/3}. \tag{2}$$

The predictions of Eq. (2) are in excellent agreement with our measurements: the power-law exponent of $1/3$ between A_{mss} and T_{mss}, the independence with the peeled length L and the weak dependence with the peel angle θ and ribbon bending modulus B through the $1/6$ exponent reproduce the various measured dependencies reported in Figs. 2 and 3. Indeed, normalizing the amplitude A_{mss} by the prefactor $\{2B/[\mu(1-\cos\theta)]\}^{1/6}$ in Eq. (2), which accounts for the changes in mass and bending modulus of the ribbon, as well as the different peel angle used, tends to gather the data on a master curve. The data collapse is particularly convincing for the samples with different backing thickness

as shown in Fig. 3. Moreover, following Eq. (2), we could fit the large amount of data reported in Fig. 2, for the various experiments performed at different (L, θ) with only one backing, to extract the free parameter d, corresponding to the critical elongation at which the glue detaches, $d = 5\ \mu$m. Such order of magnitude is compatible with our direct side observations of the adhesive tape unstable peeling. Strikingly, with this single value for d, we can finally describe quantitatively our various experiments with samples of different lineic mass μ and bending modulus B, as shown by the dashed line reported in Fig. 3.

To conclude, thanks to an extensive experimental study in addition to a careful preparation of adhesive-substrate joints with the exploration of several tape backing bending modulus, we have been able to unveil the precise characteristics of the detachment front micro-stick-slip dynamics, appearing when peeling an adhesive tape at high velocities. A local energy balance of the detachment process shows that the elastic bending energy stored in the tape region that will detach during the microslip is converted into a kinetic energy increase of the peeled tape during a micro-stick-slip cycle. Our model allows a quantitative description of the observed scaling law linking amplitudes and periods of the micro-instability, and, in particular, its dependency with the peeling angle, as well as with the bending modulus and lineic mass of the ribbon. This energy transfer arising from the assumption of the complete dissipation of the energy stored in the deformation of the adhesive layer when it detaches, by elastic hysteresis, highlights that the rapid microslip corresponds to a specific dynamic rupture mode of propagation of the detachment front. In our scenario, the elastic stretching energy stored in the whole peeled ribbon during the stick phase of the macroinstability and released during the macro-slip phase constitutes an energy reservoir for the micro-stick-slip cycles and more precisely for the reloading of the tape local bending during the microsticks. The release of the stretching energy therefore proceeds by quanta of elastic bending energy of the ribbon close to the peel front.

Nevertheless, the physical origin of the kinked detachment front propagation in the direction transverse to the main peeling direction still needs to be uncovered. A possible explanation could come from a local enhancement of the mechanical energy release rate, which has been shown [38,39] to be at the origin of the elastic fingering instability when peeling quasistatically a confined elastomer [40].

The ANR Grant "AdhesiPS" No. ANR-17-CE08-0008, the MON "MegaGrant" No. 14.W03.31.0002, and the French/Norwegian International Associated Laboratory (LIA) "D-FFRACT" supported this work.

*stephane.santucci@ens-lyon.fr

[1] J. L. Gardon, J. Appl. Polym. Sci. **7**, 625 (1963).
[2] D. W. Aubrey, G. N. Welding, and T. Wong, J. Appl. Polym. Sci. **13**, 2193 (1969).
[3] J. L. Racich and J. A. Koutsky, J. Appl. Polym. Sci. **19**, 1479 (1975).
[4] M. Barquins, B. Khandani, and D. Maugis, C.R. Acad. Sci. Ser. Gen., Ser. 2 **303**, 1517 (1986).
[5] D. Maugis and M. Barquins, *Adhesion 12*, edited by K. Allen (Elsevier ASP, London, 1988), pp. 205–222.
[6] M. Barquins and M. Ciccotti, Int. J. Adhes. Adhes. **17**, 65 (1997).
[7] G. Ryschenkow and H. Arribart, J. Adhes. **58**, 143 (1996).
[8] M. Gandur, M. Kleinke, and F. Galembeck, J. Adhes. Sci. Technol. **11**, 11 (1997).
[9] M. Ciccotti, B. Giorgini, D. Vallet, and M. Barquins, Int. J. Adhes. Adhes. **24**, 143 (2004).
[10] R. De, A. Maybhate, and G. Ananthakrishna, Phys. Rev. E **70**, 046223 (2004).
[11] P.-P. Cortet, M. Ciccotti, and L. Vanel, J. Stat. Mech. (2007) P03005.
[12] R. De and G. Ananthakrishna, Eur. Phys. J. B **61**, 475 (2008).
[13] T. Baumberger and C. Caroli, Adv. Phys. **55**, 279 (2006).
[14] S. M. Rubinstein, G. Cohen, and J. Fineberg, Nature (London) **430**, 1005 (2004).
[15] I. Svetlizky and J. Fineberg, Nature (London) **509**, 205 (2014).
[16] J. Fineberg and M. Marder, Phys. Rep. **313**, 1 (1999).
[17] S. T. Thoroddsen, H. D. Nguyen, K. Takehara, and T. G. Etoh, Phys. Rev. E **82**, 046107 (2010).
[18] J. O. Marston, P. W. Riker, and S. T. Thoroddsen, Sci. Rep. **4**, 4326 (2014).
[19] M.-J. Dalbe, P.-P. Cortet, M. Ciccotti, L. Vanel, and S. Santucci, Phys. Rev. Lett. **115**, 128301 (2015).
[20] A. Gauthier, M. Rivetti, J. Teisseire, and E Barthel, Phys. Rev. Lett. **110**, 046101 (2013).
[21] D. Hull and D. J. Bacon, *Introduction to Dislocations* (Butterworth-Heinemann, Oxford, UK, 1965).
[22] P.-P. Cortet, M.-J. Dalbe, C. Guerra, C. Cohen, M. Ciccotti, S. Santucci, and L. Vanel, Phys. Rev. E **87**, 022601 (2013).
[23] M.-J. Dalbe, S. Santucci, P.-P. Cortet, and L. Vanel, Soft Matter **10**, 132 (2014).
[24] M.-J. Dalbe, S. Santucci, L. Vanel, and P.-P. Cortet, Soft Matter **10**, 9637 (2014).
[25] M.-J. Dalbe, R. Villey, M. Ciccotti, S. Santucci, P.-P. Cortet, and L. Vanel, Soft Matter **12**, 4537 (2016).
[26] See Supplemental Material at http://link.aps.org/supplemental/10.1103/PhysRevLett.122.068005 for a sketch of the experimental set-up, as well as, typical video recordings of the unstable propagation of the detachment front during the peeling of a 3M Scotch® 600 adhesive tape.
[27] In our peel experiments with the 3M Scotch® 600 tape, the macroscopic stick-slip instability appears above a driving velocity $V_a \simeq 0.2$ m/s, and disappears above $V_d \simeq 1.5$ m/s, for a peel angle $\theta = 90°$, and a peel length $L = 50$ cm. These values are smaller than the value reported in previous experiments [19,25], due to the different preparation of the adhesive-joint substrate.
[28] V. De Zotti, Instabilité de pelage d'un ruban adhésif: Effet de l'inertie sur la dynamique multi-échelle du front de détachement. Thèse de Doctorat de l'Université de Lyon (2018).
[29] N. F. Mott, Engineering **165**, 16 (1948).
[30] A. A. Griffith, Mech. Eng. A **221**, 163 (1920).

[31] A. N. Gent and R. P. Petrich, Proc. R. Soc. A **310**, 433 (1969).
[32] D. H. Kaelble, J. Colloid Sci. **19**, 413 (1964).
[33] R. Villey, C. Creton, P.-P. Cortet, M.-J. Dalbe, T. Jet, B. Saintyves, S. Santucci, L. Vanel, D. J. Yarusso, and M. Ciccotti, Soft Matter **11**, 3480 (2015).
[34] J. Chopin, R. Villey, D. Yarusso, E. Barthel, C. Creton, and M. Ciccotti, Macromolecules **51**, 8605 (2018).
[35] R. Villey, P.-P. Cortet, C. Creton, and M. Ciccotti, Int. J. Fract. **204**, 175 (2017).
[36] C. Creton and M. Ciccotti, Rep. Prog. Phys. **79**, 046601 (2016).
[37] L. D. Landau and E. M. Lifshitz, *Theory of Elasticity* (Pergamon, New York, 1959).
[38] M. Adda-Bedia and L. Mahadevan, Proc. R. Soc. A **462**, 3233 (2006).
[39] T. Vilmin, F. Ziebert, and E. Raphael, Langmuir **26**, 3257 (2010).
[40] A. Ghatak, M. K. Chaudhury, V. Shenoy, and A. Sharma, Phys. Rev. Lett. **85**, 4329 (2000).